

## Sympathetic Cooling and Slowing of Molecules with Rydberg Atoms

Chi Zhang<sup>1,\*</sup>, Seth T. Rittenhouse<sup>2,3</sup>, Timur V. Tscherbul<sup>4</sup>, H. R. Sadeghpour<sup>3</sup>, and Nicholas R. Hutzler<sup>1</sup>

<sup>1</sup>*Division of Physics, Mathematics, and Astronomy, California Institute of Technology, Pasadena, California 91125, USA*

<sup>2</sup>*Department of Physics, the United States Naval Academy, Annapolis, Maryland 21402, USA*

<sup>3</sup>*ITAMP, Center for Astrophysics | Harvard & Smithsonian Cambridge, Massachusetts 02138, USA*

<sup>4</sup>*Department of Physics, University of Nevada, Reno, Nevada 89557, USA*



(Received 6 July 2023; accepted 5 December 2023; published 19 January 2024)

We propose to sympathetically slow and cool polar molecules in a cold, low-density beam using laser-cooled Rydberg atoms. The elastic collision cross sections between molecules and Rydberg atoms are large enough to efficiently thermalize the molecules even in a low-density environment. Molecules traveling at 100 m/s can be stopped in under 30 collisions with little inelastic loss. Our method does not require photon scattering from the molecules and can be generically applied to complex species for applications in precision measurement, quantum information science, and controlled chemistry.

DOI: [10.1103/PhysRevLett.132.033001](https://doi.org/10.1103/PhysRevLett.132.033001)

Cold and trapped molecules represent promising quantum systems for a multitude of applications ranging from a table-top search of new physics beyond the standard model [1–7] to quantum information processing [8–13], which benefit from rich internal molecular structures. Recent measurements of the electron electric dipole moment [4,5], which rely on the strong internal electric field and the high-level control of molecule orientation, have constrained charge-parity violating new physics to  $\gtrsim 50$  TeV energy scales. In addition, the molecular rotational structure provides tunable long-range dipole-dipole interaction in ground electronic states [14], and may accommodate one error-corrected qubit in each molecule [15], thereby significantly reducing the number of physical qubits in a quantum information processor.

Laser cooling of molecules [16–21] and assembling ultracold atoms [22,23] are two of the main pathways to trapping molecules in the quantum regime, key to the next generations of new physics searches [24–28], long-lived qubits, and high-fidelity quantum gates. However, both methods require specific molecular structures, which limit the choice of molecules. Furthermore, laser cooling needs  $10^4$ – $10^5$  photon scattering events and thus demands high precision spectroscopy, which is challenging and time-consuming for many heavy-atom containing [29,30] or large polyatomic molecules [31,32].

Molecules can also be cooled by collisions or interactions with another species. For example, in a cryogenic buffer gas beam (CBGB) [33], cold helium gas thermalizes any molecular species to a few Kelvin temperature. Once in a trap, the molecules can be further cooled by optoelectrical Sisyphus cooling [34] or via sympathetic cooling with laser-cooled atoms [35–40]. It would be advantageous to use laser-cooled species to sympathetically cool species in lower-density environments, such as in beams, since

loading complex, reactive species into traps with sufficient atom and molecular density for efficient sympathetic cooling is often a challenge.

Here, we propose a method to slow and cool polar molecules from a CBGB, load them into a trap, and cool to ultracold temperatures, without photon scattering from the molecule. Our method has two requirements, which we will show to be generic for polar molecules. First, we require a mean free path which is short compared to the size of the atomic cloud, so that the molecules are thermalized before diffusing out of the cloud. This requires a deep atom-molecule interaction potential that is comparable to or larger than the collision energy in a CBGB. Unlike at room temperature where the molecule-Rydberg atom collision cross sections vanish [41,42], in a CBGB the center of mass collision velocity is  $\sim 10$  m/s, which corresponds to  $\sim h \times 10$  GHz for heavy molecules of  $\sim 200$  atomic mass units, where  $h$  is Planck's constant. Second, we require that the loss probability during collisions is not too high. We will show that fewer than  $\sim 30$  collisions are needed to bring a molecule from a few Kelvin and  $\sim 100$  m/s forward velocity to ultracold temperature in a trap. This requirement is much less stringent than those imposed by the previous proposals of sympathetic cooling [35–39], and we shall show that the loss probability per collision is sufficiently low in the general case.

When a molecule is outside of a Rydberg atom, the dominant interaction is the dipole-dipole interaction [43]. This interaction has been used to detect and manipulate the state of the molecule [44–46], and has been proposed for cooling trapped molecules in  $\sim$ mK temperature regime [47,48] and for entangling molecules in optical tweezers [49–51]. However, the dipole-dipole interaction is  $\ll h \times 100$  MHz  $\approx k_B \times 5$  mK, where  $k_B$  is Boltzmann's constant. This is negligible compared to the collision

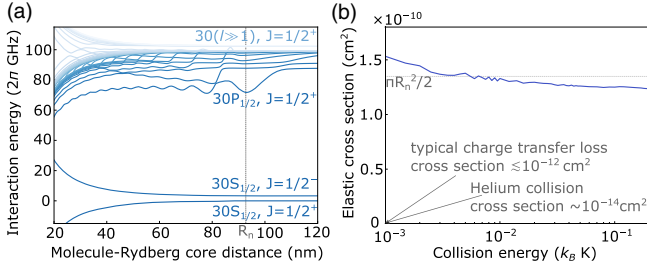


FIG. 1. (a) Interaction potential between the CH molecule and the Li Rydberg atom. The state labels indicate the asymptotic states when the molecule is far away from the Rydberg atom. When they are close, all atom-molecule pair states are hybridized. The dashed vertical line marks the classic radius of the Li( $30S_{1/2}$ ) state. When the pair state density is high near the degenerate manifold of high angular momentum Rydberg states, the interaction potential depth is larger than  $\sim 10$  GHz. (b) The scattering cross section for the potential of the  $30S_{1/2}, J = 1/2^-$  pair state, compared with the half of the cross section of a hard sphere with radius  $R_n$  ( $\pi R_n^2$ ).

energy in the  $\sim$ K temperature regime, which is of interest in this work.

The picture changes drastically when the molecule is near the edge or inside the Rydberg wave function, where the separation between the molecule and the Rydberg core  $R$  is comparable to or smaller than the electron-core distance  $r$ , and the electron can be very close to the molecule. As a result, the dominant perturbation of the molecule on the Rydberg atom comes from the charge-dipole interaction with the Rydberg electron,  $H_I = ed/|R - r|^2$  with  $d$  the molecule frame dipole moment. This interaction has been intensively studied in systems of ultralong range Rydberg molecules [52–58]. It couples and hence shifts the atom-molecule pair states strongly. The coupling strength is proportional to  $d$  and the electron’s probability density which scales as  $(n^*)^{-3}$ , with  $n^*$  the effective principal quantum number.

In Fig. 1(a), we show the interaction potentials between the CH molecule ( $d \approx 1.46D$ ) and the Li Rydberg atom as an example. We choose this atom-molecule pair since the small dipole moment of the molecule enables accurate computations; however, this method generalizes to more complex species (such as molecules with dipole moments greater than the Fermi-Teller critical dipole  $d \gtrsim 1.6D$  [59]) for which exact calculations might be impractical (see the Supplemental Material [60] for details). For the near-degenerate manifold of high angular momentum states, the pair states are well hybridized and the potentials are  $\sim 10$  GHz deep. The potentials for the  $S$  Rydberg states are weaker but still exceed GHz inside the Rydberg radius.

The range of the  $\gtrsim$ GHz potential is similar to the radius of the Rydberg wave function  $R_n \approx 2(n^*)^2 a_0$ , where  $a_0$  is the Bohr radius. The relative collision velocity (in the center of mass frame) in a CBGB is  $\lesssim 10$  m/s, which

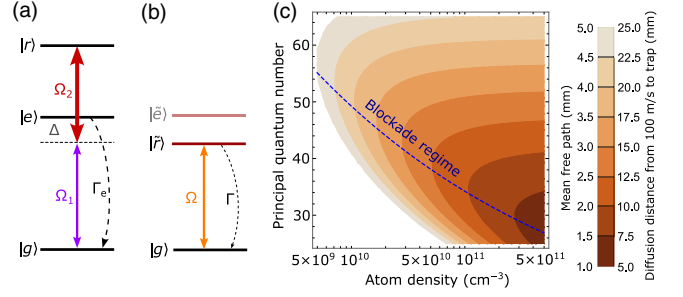


FIG. 2. (a) and (b) Laser coupling scheme for Rydberg excitation and cooling.  $\Omega_2$  (red arrow) couples  $|e\rangle \leftrightarrow |r\rangle$  off resonantly, and  $\Omega_1$  (purple arrow) couples  $|g\rangle$  to the dressed Rydberg state  $|\tilde{r}\rangle$  with an effective coupling strength  $\Omega \approx 2\pi \times 1$  MHz (orange arrow in [b]). (c) Mean free path of the collision, as well as the diffusion distance (in the atom cloud) to stop a molecule initially at 100 m/s, as a function of the total atom density (Rydberg and ground states) and principal quantum number, when the system is in a steady state with the laser couplings in (a). We use 25 as the number of collisions needed to stop the molecules, as described in the main text. The blue dashed line marks the parameters above which the blockade effect starts to limit the Rydberg population density.

roughly corresponds to  $\lesssim \hbar \times 0.5$  GHz collision energy for the CH molecule and the Li atom. This is much less than the potential depth; therefore the cross section is expected to be nearly the size of the potential,  $\sim \pi R_n^2$ . Even for heavier molecules with up to  $\sim 200$  atomic mass units, the  $\sim \hbar \times 10$  GHz deep potentials are also sufficient for large cross sections. As an example, the scattering cross section of CH and Li is calculated and plotted in Fig. 1(b). For  $n^* \approx 30$ , the cross section is around 4 orders of magnitude larger than that of the helium atom, the most common buffer gas. This large cross section enables a short mean free path even in the dilute beam outside of the buffer gas cell.

This enhancement of collision cross section is general, and can be used for a variety of experimental goals. We now discuss a specific approach to implementing this method to slow, stop, trap, and cool molecules from a CBGB without laser cooling them. In a cloud of atoms, we consider the laser coupling scheme shown in Fig. 2(a) for Rydberg excitation and for Zeeman slowing of the atom. The scheme is conceptually similar to electromagnetically induced transparency cooling [61,62], in which the excited state is coupled to an intermediate state, and this dressed superposition state is used as an effective excited state for photon cycling; more details are in the Supplemental Material [60]. The excited state  $|e\rangle$  and Rydberg state  $|r\rangle$  are coupled by a blue detuned Rydberg laser with coupling strength  $\Omega_2$  and detuning  $\Delta$ ; the dressed eigenstate with dominant Rydberg character is  $|\tilde{r}\rangle = \cos\theta|r\rangle - \sin\theta|e\rangle$ , with the mixing angle  $\theta$  given by  $\tan 2\theta = -\Omega_2/\Delta$ . We consider  $\Delta \gg \Omega_2 > \Gamma_e$ , as the Rydberg state linewidths ( $\lesssim 100$  kHz) are much less than the low-lying excited state

linewidth; therefore the linewidth of the dressed Rydberg state  $|\tilde{r}\rangle$  is dominated by the contribution from  $|e\rangle$ , and it primarily decays directly to the ground state  $|g\rangle$  and allows for fast photon cycling (population in  $|r\rangle$  decays indirectly to the ground state within  $\sim 10 \mu\text{s}$ ; see the Supplemental Material [60]). For most alkali ( $\Gamma_e \approx 2\pi \times 5 \text{ MHz}$ ) and alkaline earth ( $\Gamma_e \approx 2\pi \times 30 \text{ MHz}$ ) atoms, the  $|\tilde{r}\rangle$  state linewidth  $\Gamma$  can be tuned to around  $2\pi \times 1 \text{ MHz}$  by mixing a few percent or less  $|e\rangle$  population. The effective coupling  $|g\rangle \leftrightarrow |\tilde{r}\rangle$  can be tuned to around  $\Omega \approx \Omega_1 \Omega_2 / 2\Delta = 2\pi \times 1 \text{ MHz}$ , yielding a value for the saturation parameter  $s = [(\Omega^2/2)/(\Delta^2 + \Gamma^2/4)] \approx 1$ .

These parameters are suitable for most alkali and alkaline earth atoms. The timescale of an oscillation between  $|g\rangle \leftrightarrow |\tilde{r}\rangle$  is much longer than the collision time ( $\ll 0.1 \mu\text{s}$ , the time during which the molecule is inside the Rydberg wave function). In the Zeeman slower, the cooling laser  $\Omega_1$  is counterpropagating to the atoms traveling direction, and the Rydberg laser  $\Omega_2$  is from the opposite side with an angle to match the  $k$ -vector projections of  $\Omega_1$  and  $\Omega_2$  on the atomic beam direction (see the Supplemental Material [60]). As a result, their Doppler shifts on  $|g\rangle \leftrightarrow |e\rangle$  and  $|e\rangle \leftrightarrow |r\rangle$  transitions are opposite. A position-dependent magnetic field shifts  $|e\rangle$  (typically a  $P$  state) differently from  $|g\rangle$  and  $|r\rangle$  ( $S$  states) and thus can compensate the opposite Doppler shifts in  $|g\rangle \leftrightarrow |e\rangle$  and  $|e\rangle \leftrightarrow |r\rangle$  simultaneously. As a result, the Rydberg excitation scheme is not affected by the Zeeman slower for the target velocity class, and we can slow the atomic beam while maintaining a fixed Rydberg excitation fraction.

In steady state with these couplings, the mean free path,  $l \approx (\sigma\rho)^{-1}$  where  $\sigma$  is the elastic collision cross section and  $\rho$  is the Rydberg atom density, is calculated and plotted in Fig. 2(b) as a function of total atom density (in both ground and Rydberg states) and principal quantum number. For low Rydberg states the dressed Rydberg population can reach 25% (for  $s = 1$ ), while for high Rydberg states it is limited by the Rydberg blockade effect [43,72]. The blue dashed line marks the parameters where the Rydberg blockade starts to limit the density of atoms in Rydberg states. The collision cross section scales geometrically as  $(n^*)^4$ , until the interaction potential is too weak, but the probability of Rydberg excitation can be suppressed by the Rydberg blockade, which scales as  $(n^*)^7$ . As a result, the optimal density and principal quantum number are near the blockade regime.

An example of the experimental sequence is shown in Fig. 3. The density of atoms made inside the buffer gas cell is typically  $10^{13}\text{--}10^{14} \text{ cm}^{-3}$  [33]. After exiting the cell, the density decreases rapidly because of expansion and collision with the buffer gas. We propose to first laser cool the atoms in all three dimensions to stop the expansion and keep the density high. The cooling needs to be in the moving frame to maintain the overlap between cooled atoms and uncooled molecules before subsequent Rydberg

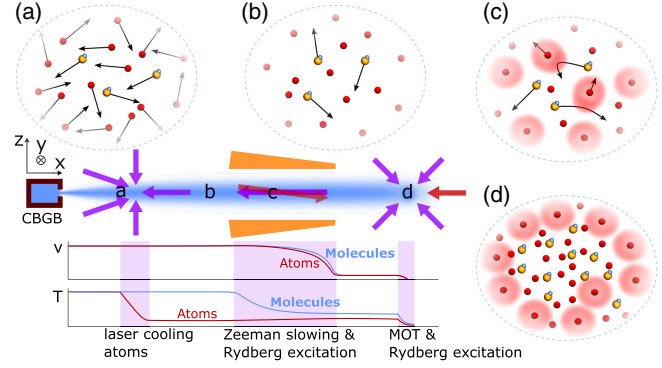


FIG. 3. Proposed experimental setup and sequence. A beam (blue) of atoms and molecules comes out from a buffer gas cell (brown box). The plots qualitatively illustrate the expected temperature ( $T$ ) and velocity ( $v$ ) profiles of the atoms and molecules. In (a), atoms and molecules are both relatively hot (typically  $\sim 4 \text{ K}$ ) and fast (typically  $\sim 100 \text{ m/s}$  [33]). Laser cooling is applied to the atoms in the moving frame. The frequencies of the beams along the  $x$  direction are shifted for cooling in the moving frame. Two beams in the  $y$  direction are not shown in the figure. After cooling, in (b), atoms are cold ( $< 100 \mu\text{K}$ ), but molecules are still hot. In the Zeeman slower (orange), atoms are excited to the dressed Rydberg state  $|\tilde{r}\rangle$  by two counterpropagating beams. In (c), molecules collide and thermalize with the Rydberg atoms and are cooled to the steady state temperature ( $\sim 100 \text{ mK}$ ). After slowing, magneto-optical force and position-dependent Rydberg excitation are applied to compress the density of the molecules and load them into a trap. (d) The magneto-optical trap where the molecules are pushed by the Rydberg atoms toward the center of the trap.

excitation (for collisions). At around  $100 \text{ mm}$  outside the cell downstream the atom density is  $10^{10}$  or  $10^{11} \text{ cm}^{-3}$ , and the buffer gas collision rate is low enough for laser cooling. At this position, where the sympathetic cooling begins, the range of typical molecule densities is  $10^8\text{--}10^9 \text{ cm}^{-3}$  [33]. Cooling in the moving frame can be achieved by detuning the longitudinal cooling laser frequencies.

Typical polarization gradient cooling, after a two-dimensional magneto-optical trap, can lower the temperature of the atoms to  $T_A < 100 \mu\text{K}$  within a few  $\text{cm}$  [73], and then the atom density will stay at  $10^{10}\text{--}10^{11} \text{ cm}^{-3}$ . Subsequently, the cloud of ultracold atoms and uncooled molecules enters the Zeeman slower, where the atoms are excited to  $|\tilde{r}\rangle$  for both slowing and collisions. The mean acceleration on the atoms is  $a \approx [(s/2)/(1+s)][(h\Gamma)/(m_A\lambda)]$ , where  $m_A$  is the mass of the atom and  $\lambda$  is the wavelength of the transition. During the slowing process, molecules are also slowed by collisions with Rydberg atoms. In the moving frame of the ultracold atoms, the molecules have initial kinetic energies of  $\sim 1 \text{ K}$  and are constantly accelerated by  $a$ , relative to the atoms until the cloud is stopped. The optimal mean free path  $l$  can reach 2 to 3  $\text{mm}$  [see Fig. 2(b)]. For atoms and molecules with similar masses, the expected molecule kinetic energy after one collision is  $T_{M,f} \approx (T_{M,i} + T_A)/2$ , where  $T_{M,i}$

is the kinetic energy before the collision. We assume the atoms are not heated up by the collisions since there are typically at least 2 orders of magnitude more atoms than molecules [33]. In steady state, the kinetic energy loss of the molecules in the collision  $T_{M,i} - T_{M,f} \approx T_{M,f}$  is similar to the kinetic energy gained between two successive collisions by acceleration  $m_M a l$ , with  $m_M$  the molecule mass (and  $m_M \approx m_A$ ). Therefore, the collision energy  $T_{M,i} \approx 2m_M a l \approx [s/(1+s)](l/\lambda)h\Gamma$ . The collision energy is independent of the mass, and for the typical parameters we choose ( $s \approx 1$ ,  $\Gamma \approx 2\pi \times 1$  MHz) it is around  $h \times 2$  GHz ( $\approx k_B \times 100$  mK), which is low enough for the interaction potential between most polar molecules and Rydberg states, though it can be further reduced by using smaller  $s$  or  $\Gamma$ . The laser slowing distance of the entire cloud is  $v^2/(2a)$ , which is proportional to the atom mass, is 0.5 m for heavy atoms with  $\sim 200$  atomic mass unit, and has an initial velocity of 100 m/s. During the slowing process, on average a molecule collides  $N \approx 25$  times with Rydberg atoms (within the first five collisions the molecules initially at 1 K can reach the steady state). This leads to a diffusion distance of  $l\sqrt{N} \approx 1$  cm [shown in Fig. 2(b)], which is less than the typical size of the ultracold atomic cloud ( $\sim 3$  cm). On average, half of the molecules in the  $\approx 1$  cm outer shell of the cloud may diffuse out. This results in a  $\lesssim 30\%$  loss assuming uniform initial distribution. Although we assume the initial forward velocity is  $\sim 100$  m/s, we note that slow beams with  $< 50$  m/s from CBGB have been experimentally demonstrated [31,74,75]; this allows for a shorter Zeeman slower and thus less diffusion loss.

After Zeeman slowing, the molecules can be loaded into a magnetic trap [36,76], or any other trap which is sufficiently deep. If further cooling is needed, the molecules could be directly laser cooled if they can scatter a sufficient number of photons, though now with less stringent requirements on vibrational closure due to the fact that they are now already stopped.

Alternatively we propose a method to capture and cool both the atoms and molecules with a magneto-optical trap (MOT) after the Zeeman slower but without scattering photons from the molecules. Atoms are excited to  $|\tilde{r}\rangle$  (see Fig. 2) on the edge of the MOT, which provides a position-dependent force to confine the atoms. This can be achieved by a position-dependent magnetic field, in which the transition frequency is shifted (including different magnetic sublevels if needed), and uniform laser fields. Molecules can collide with the shell of Rydberg atoms ( $|\tilde{r}\rangle$ ) so that they are confined and further thermalized. In the meantime, as we slowly vary the frequencies of the lasers and shrink the Rydberg shell, the molecular density is compressed.

After  $N$  more collisions, the molecules have temperature  $T_M(N) \approx T_A + T_M(0)e^{-N/2}$ , where  $T_M(0) \approx 100$  mK is the steady state molecule energy after Zeeman slowing. Within around 10 collisions, the molecules are thermalized to  $\lesssim 1$  mK. The shell thickness is determined by the

linewidth of  $|\tilde{r}\rangle$  and the magnetic field gradient. We need a large MOT [77] with a thick shell of Rydberg atoms, for instance  $d \approx 1$  cm. The probability of molecules inside the shell diffusing out during the compression is  $(1 - e^{-\sqrt{N}l/d})/2 \approx 20\%$ . After the compression, the molecules can be loaded into an optical dipole, magnetic, or other trap.

By leveraging the large elastic cross sections between molecules and Rydberg atoms, we propose a new approach to slow, trap, and cool molecules to ultracold temperatures without scattering photons from the molecule. However, there can be unwanted side effects of *inelastic* collisions, including ion-molecule chemical reaction, rotational state changes, and charge transfer. We argue that these are unlikely to be major limitations.

First, when the molecule is inside the Rydberg wave function, it can be attracted by the ion core and react chemically at short distances. This effect has been studied at low energies in Ref. [63] in collisions between polar molecules and Rydberg atoms. It is shown in Ref. [63] that the state of the molecule evolves adiabatically, and only molecules in a small subset of strong-field seeking states react with the ion core. As a result, molecules in the weak-field seeking states are not subject to this loss mechanism (see the Supplemental Material [60]). Second, there could be charge transfer collisions [78], whereby the Rydberg electron migrates from the atom to the molecule. These collisions have been studied both theoretically and experimentally [79–84], and have been observed to be significant for molecules with  $d > 2.5D$  dipole moments. Furthermore, the cross section depends on the principal quantum number and normally has a peak. At several principal quantum numbers away from the peak, the charge transfer loss cross section is typically  $\ll 10^{-12}$  cm<sup>2</sup>, more than 2 orders of magnitude smaller than the elastic cross section. As a result, the inelastic collisions should have negligible loss effects, and more than half of the molecules from the 100 m/s distribution should survive in an ultracold trap, making Rydberg atom sympathetic cooling more efficient than laser cooling with only a  $10^{-5}$  photon-scattering leakage.

In summary, we have proposed that polar molecules can be slowed and cooled by collisions with laser cooled Rydberg atoms. Our method does not require scattering photons from the molecule, and the interaction with the Rydberg atom arises from the molecular dipole moment, and as such, the method works generically for polar molecules. Our method provides a pathway into traps at ultracold temperatures for many molecules that do not have laser cycling transitions or that are hard to cool. This will significantly boost a host of applications using ultracold molecules, such as quantum information and table-top searches for new physics.

The authors would like to thank Rosario Gonzalez-Ferez for preliminary calculations in the early stages of this work.

We thank Yi Zeng, Ashay Patel, Weibin Li, Lan Cheng, Tim Steimle, Zack Lasner, Mike Tarbutt, and Gerard Higgins for helpful discussions. The work at Caltech has been supported by the Gordon and Betty Moore Foundation Grant No. GBMF7947 and Alfred P. Sloan Foundation Grant No. G-2019-12502. C. Z. acknowledges support from the David and Ellen Lee Postdoctoral Fellowship at Caltech. T. V. T. gratefully acknowledges support from the NSF CAREER Grant No. PHY-2045681. H. R. S. acknowledges support from the NSF through a grant for ITAMP at Harvard University.

\*chizhang@caltech.edu

- [1] M. S. Safronova, D. Budker, D. DeMille, D. F. Jackson Kimball, A. Derevianko, and C. W. Clark, *Rev. Mod. Phys.* **90**, 025008 (2018).
- [2] J. J. Hudson, D. M. Kara, I. J. Smallman, B. E. Sauer, M. R. Tarbutt, and E. A. Hinds, *Nature (London)* **473**, 493 (2011).
- [3] J. Baron, W. C. Campbell, D. DeMille, J. M. Doyle, G. Gabrielse, Y. V. Gurevich, P. W. Hess, N. R. Hutzler, E. Kirilov, I. Kozyryev, B. R. O'Leary, C. D. Panda, M. F. Parsons, E. S. Petrik, B. Spaun, A. C. Vutha, and A. D. West, *Science* **343**, 269 (2014).
- [4] V. Andreev, D. G. Ang, D. DeMille, J. M. Doyle, G. Gabrielse, J. Haefner, N. R. Hutzler, Z. Lasner, C. Meisenhelder, B. R. O'Leary, C. D. Panda, A. D. West, E. P. West, and X. Wu, *Nature (London)* **562**, 355 (2018).
- [5] T. S. Roussy, L. Caldwell, T. Wright, W. B. Cairncross, Y. Shagam, K. B. Ng, N. Schlossberger, S. Y. Park, A. Wang, J. Ye, and E. A. Cornell, *Science* **381**, 46 (2023).
- [6] S. Truppe, R. J. Hendricks, S. K. Tokunaga, H. J. Lewandowski, M. G. Kozlov, C. Henkel, E. A. Hinds, and M. R. Tarbutt, *Nat. Commun.* **4**, 2600 (2013).
- [7] K. H. Leung, B. Iritani, E. Tiberi, I. Majewska, M. Borkowski, R. Moszynski, and T. Zelevinsky, *Phys. Rev. X* **13**, 011047 (2023).
- [8] C. M. Holland, Y. Lu, and L. W. Cheuk, *arXiv:2210.06309*.
- [9] Y. Bao, S. S. Yu, L. Anderegg, E. Chae, W. Ketterle, K.-K. Ni, and J. M. Doyle, *arXiv:2211.09780*.
- [10] Y. Lin, D. R. Leibbrandt, D. Leibfried, and C.-w. Chou, *Nature (London)* **581**, 273 (2020).
- [11] J. W. Park, Z. Z. Yan, H. Loh, S. A. Will, and M. W. Zwierlein, *Science* **357**, 372 (2017).
- [12] P. D. Gregory, J. A. Blackmore, S. L. Bromley, J. M. Hutson, and S. L. Cornish, *Nat. Phys.* **17**, 1149 (2021).
- [13] S. Burchesky, L. Anderegg, Y. Bao, S. S. Yu, E. Chae, W. Ketterle, K.-K. Ni, and J. M. Doyle, *Phys. Rev. Lett.* **127**, 123202 (2021).
- [14] J. A. Blackmore, L. Caldwell, P. D. Gregory, E. M. Bridge, R. Sawant, J. Aldegunde, J. Mur-Petit, D. Jaksch, J. M. Hutson, B. E. Sauer, M. R. Tarbutt, and S. L. Cornish, *Quantum Sci. Technol.* **4**, 014010 (2019).
- [15] V. V. Albert, J. P. Covey, and J. Preskill, *Phys. Rev. X* **10**, 031050 (2020).
- [16] J. F. Barry, D. J. McCarron, E. B. Norrgard, M. H. Steinecker, and D. DeMille, *Nature (London)* **512**, 286 (2014).
- [17] S. Truppe, H. J. Williams, M. Hambach, L. Caldwell, N. J. Fitch, E. A. Hinds, B. E. Sauer, and M. R. Tarbutt, *Nat. Phys.* **13**, 1173 (2017).
- [18] L. W. Cheuk, L. Anderegg, B. L. Augenbraun, Y. Bao, S. Burchesky, W. Ketterle, and J. M. Doyle, *Phys. Rev. Lett.* **121**, 083201 (2018).
- [19] L. Caldwell, J. A. Devlin, H. J. Williams, N. J. Fitch, E. A. Hinds, B. E. Sauer, and M. R. Tarbutt, *Phys. Rev. Lett.* **123**, 033202 (2019).
- [20] S. Ding, Y. Wu, I. A. Finneran, J. J. Burau, and J. Ye, *Phys. Rev. X* **10**, 021049 (2020).
- [21] T. K. Langin, V. Jorapur, Y. Zhu, Q. Wang, and D. DeMille, *Phys. Rev. Lett.* **127**, 163201 (2021).
- [22] K.-K. Ni, S. Ospelkaus, M. H. G. de Miranda, A. Pe'er, B. Neyenhuis, J. J. Zirbel, S. Kotochigova, P. S. Julienne, D. S. Jin, and J. Ye, *Science* **322**, 231 (2008).
- [23] L. D. Marco, G. Valtolina, K. Matsuda, W. G. Tobias, J. P. Covey, and J. Ye, *Science* **363**, 853 (2019).
- [24] X. Alauze, J. Lim, M. A. Trigatzis, S. Swarbrick, F. J. Collings, N. J. Fitch, B. E. Sauer, and M. R. Tarbutt, *Quantum Sci. Technol.* **6**, 044005 (2021).
- [25] N. J. Fitch, J. Lim, E. A. Hinds, B. E. Sauer, and M. R. Tarbutt, *Quantum Sci. Technol.* **6**, 014006 (2020).
- [26] B. L. Augenbraun, Z. D. Lasner, A. Frenett, H. Sawaoka, C. Miller, T. C. Steimle, and J. M. Doyle, *New J. Phys.* **22**, 022003 (2020).
- [27] I. Kozyryev and N. R. Hutzler, *Phys. Rev. Lett.* **119**, 133002 (2017).
- [28] T. A. Isaev, S. Hoekstra, and R. Berger, *Phys. Rev. A* **82**, 052521 (2010).
- [29] C. Zhang, C. Zhang, L. Cheng, T. C. Steimle, and M. R. Tarbutt, *J. Mol. Spectrosc.* **386**, 111625 (2022).
- [30] T. D. Persinger, J. Han, A. T. Le, T. C. Steimle, and M. C. Heaven, *Phys. Rev. A* **106**, 062804 (2022).
- [31] B. L. Augenbraun, L. Anderegg, C. Hallas, Z. D. Lasner, N. B. Vilas, and J. M. Doyle, *Adv. At. Mol. Opt. Phys.* **72**, 89 (2023).
- [32] D. Mitra, Z. D. Lasner, G.-Z. Zhu, C. E. Dickerson, B. L. Augenbraun, A. D. Bailey, A. N. Alexandrova, W. C. Campbell, J. R. Caram, E. R. Hudson, and J. M. Doyle, *J. Phys. Chem. Lett.* **13**, 7029 (2022).
- [33] N. R. Hutzler, H. I. Lu, and J. M. Doyle, *Chem. Rev.* **112**, 4803 (2012).
- [34] A. Prehn, M. Ibrügger, R. Glöckner, G. Rempe, and M. Zeppenfeld, *Phys. Rev. Lett.* **116**, 063005 (2016).
- [35] J. Lim, M. D. Frye, J. M. Hutson, and M. R. Tarbutt, *Phys. Rev. A* **92**, 053419 (2015).
- [36] S. Jurgilas, A. Chakraborty, C. J. H. Rich, L. Caldwell, H. J. Williams, N. J. Fitch, B. E. Sauer, M. D. Frye, J. M. Hutson, and M. R. Tarbutt, *Phys. Rev. Lett.* **126**, 153401 (2021).
- [37] R. Rugango, J. E. Goeders, T. H. Dixon, J. M. Gray, N. B. Khanyile, G. Shu, R. J. Clark, and K. R. Brown, *New J. Phys.* **17**, 035009 (2015).
- [38] T. V. Tschersbul, J. Kłos, and A. A. Buchachenko, *Phys. Rev. A* **84**, 040701(R) (2011).
- [39] M. Morita, J. Kłos, A. A. Buchachenko, and T. V. Tschersbul, *Phys. Rev. A* **95**, 063421 (2017).
- [40] H. Son, J. J. Park, W. Ketterle, and A. O. Jamison, *Nature (London)* **580**, 197 (2020).

- [41] R. Stebbings and F. Dunning, *Rydberg States of Atoms and Molecules*, Essays in Nuclear Astrophysics (Cambridge University Press, Cambridge, England, 1983).
- [42] T. F. Gallagher, *Rydberg Atoms*, Cambridge Monographs on Atomic, Molecular and Chemical Physics (Cambridge University Press, Cambridge, England, 1994).
- [43] E. Urban, T. A. Johnson, T. Henage, L. Isenhower, D. D. Yavuz, T. G. Walker, and M. Saffman, *Nat. Phys.* **5**, 110 (2009).
- [44] S. Patsch, M. Zeppenfeld, and C. P. Koch, *J. Phys. Chem. Lett.* **13**, 10728 (2022).
- [45] V. Zhelyazkova and S. D. Hogan, *Phys. Rev. A* **95**, 042710 (2017).
- [46] F. Jarisch and M. Zeppenfeld, *New J. Phys.* **20**, 113044 (2018).
- [47] S. D. Huber and H. P. Büchler, *Phys. Rev. Lett.* **108**, 193006 (2012).
- [48] B. Zhao, A. W. Glaetzle, G. Pupillo, and P. Zoller, *Phys. Rev. Lett.* **108**, 193007 (2012).
- [49] C. Zhang and M. R. Tarbutt, *PRX Quantum* **3**, 030340 (2022).
- [50] K. Wang, C. P. Williams, L. R. B. Picard, N. Y. Yao, and K.-K. Ni, *PRX Quantum* **3**, 030339 (2022).
- [51] E. Kuznetsova, S. T. Rittenhouse, H. R. Sadeghpour, and S. F. Yelin, *Phys. Chem. Chem. Phys.* **13**, 17115 (2011).
- [52] A. Guttridge, D. K. Ruttley, A. C. Baldock, R. González-Férez, H. R. Sadeghpour, C. S. Adams, and S. L. Cornish, *Phys. Rev. Lett.* **131**, 013401 (2023).
- [53] S. T. Rittenhouse and H. R. Sadeghpour, *Phys. Rev. Lett.* **104**, 243002 (2010).
- [54] S. T. Rittenhouse, M. Mayle, and P. Schmelcher, and H. Sadeghpour, *J. Phys. B* **44**, 184005 (2011).
- [55] J. P. Shaffer, S. T. Rittenhouse, and H. R. Sadeghpour, *Nat. Commun.* **9**, 1965 (2018).
- [56] R. González-Férez, H. Sadeghpour, and P. Schmelcher, *New J. Phys.* **17**, 013021 (2015).
- [57] J. Aguilera-Fernández, H. R. Sadeghpour, P. Schmelcher, and R. González-Férez, *Phys. Rev. A* **96**, 052509 (2017).
- [58] R. González-Férez, J. Shertzer, and H. R. Sadeghpour, *Phys. Rev. Lett.* **126**, 043401 (2021).
- [59] E. Fermi and E. Teller, *Phys. Rev.* **72**, 399 (1947).
- [60] See Supplemental Material at <http://link.aps.org/supplemental/10.1103/PhysRevLett.132.033001> for details about the molecule-Rydberg atom interaction, the laser cooling scheme, and the inelastic collisions, which includes Ref. [21,33,53,54,56,58,61–71].
- [61] G. Morigi, J. Eschner, and C. H. Keitel, *Phys. Rev. Lett.* **85**, 4458 (2000).
- [62] R. Lechner, C. Maier, C. Hempel, P. Jurcevic, B. P. Lanyon, T. Monz, M. Brownnutt, R. Blatt, and C. F. Roos, *Phys. Rev. A* **93**, 053401 (2016).
- [63] V. Zhelyazkova, F. B. V. Martins, J. A. Agner, H. Schmutz, and F. Merkt, *Phys. Rev. Lett.* **125**, 263401 (2020).
- [64] M. Mayle, S. T. Rittenhouse, P. Schmelcher, and H. R. Sadeghpour, *Phys. Rev. A* **85**, 052511 (2012).
- [65] E. Kuznetsova, S. T. Rittenhouse, H. R. Sadeghpour, and S. F. Yelin, *Phys. Rev. A* **94**, 032325 (2016).
- [66] J. E. Turner, *Am. J. Phys.* **45**, 758 (1977).
- [67] P. Giannakeas, M. T. Eiles, F. Robicheaux, and J. M. Rost, *Phys. Rev. Lett.* **125**, 123401 (2020).
- [68] A. Messiah, *Quantum Mechanics* (Dover, New York, 2014).
- [69] C. J. Ho, J. A. Devlin, I. M. Rabey, P. Yzombard, J. Lim, S. C. Wright, N. J. Fitch, E. A. Hinds, M. R. Tarbutt, and B. E. Sauer, *New J. Phys.* **22**, 043031 (2020).
- [70] S. C. Wright, M. Doppelbauer, S. Hofsäuss, H. C. Schewe, B. Sartakov, G. Meijer, and S. Truppe, *Mol. Phys.* **121**, e2146541 (2022).
- [71] T. K. Langin and D. DeMille, *New J. Phys.* **25**, 043005 (2023).
- [72] A. Gaëtan, Y. Miroshnychenko, T. Wilk, A. Chotia, M. Viteau, D. Comparat, P. Pillet, A. Browaeys, and P. Grangier, *Nat. Phys.* **5**, 115 (2009).
- [73] J. A. Devlin and M. R. Tarbutt, *New J. Phys.* **18**, 123017 (2016).
- [74] B. L. Augenbraun, A. Frenett, H. Sawaoka, C. Hallas, N. B. Vilas, A. Nasir, Z. D. Lasner, and J. M. Doyle, *Phys. Rev. Lett.* **127**, 263002 (2021).
- [75] H. Sawaoka, A. Frenett, A. Nasir, T. Ono, B. L. Augenbraun, T. C. Steimle, and J. M. Doyle, *Phys. Rev. A* **107**, 022810 (2023).
- [76] D. J. McCarron, M. H. Steinecker, Y. Zhu, and D. DeMille, *Phys. Rev. Lett.* **121**, 013202 (2018).
- [77] A. Camara, R. Kaiser, and G. Labeyrie, *Phys. Rev. A* **90**, 063404 (2014).
- [78] S. Markson and H. R. Sadeghpour, *J. Phys. B* **49**, 114006 (2016).
- [79] C. Desfrancois, H. Abdoul-Carime, N. Khelifa, and J. P. Schermann, *Phys. Rev. Lett.* **73**, 2436 (1994).
- [80] M. Matsuzawa, *J. Phys. B* **8**, 2114 (1975).
- [81] M. Hamamda, P. Pillet, H. Lignier, and D. Comparat, *New J. Phys.* **17**, 045018 (2015).
- [82] E. Y. Buslov and B. A. Zon, *Phys. Rev. A* **85**, 042709 (2012).
- [83] V. S. Lebedev and A. A. Narits, *Chem. Phys. Lett.* **582**, 10 (2013).
- [84] C.-H. Qian, G.-Z. Zhu, and L.-S. Wang, *J. Phys. Chem. Lett.* **10**, 6472 (2019).